Developmental Biology 328 (2009) 200–209

Contents lists available at ScienceDirect

Developmental Biology

journal homepage: www.elsevier.com/developmentalbiology

Functional equivalence of the zinc finger transcription factors Osr1 and Osr2 in mouse development

Yang Gao, Yu Lan, Catherine E. Ovitt, Rulang Jiang *

Department of Biomedical Genetics and Center for Oral Biology, University of Rochester School of Medicine and Dentistry, Rochester, NY 14642, USA

ARTICLE INFO

Article history:
Received for publication 7 July 2008
Revised 6 January 2009
Accepted 6 January 2009
Available online 14 January 2009

Keywords:
Cleft palate
Eyelid development
Fgf10, Functional equivalence
Gene substitution
Knockin
Odd-skipped
Osr1
Osr2
Palate development

ABSTRACT

Osr1 and Osr2 are the only mammalian homologs of the *Drosophila* odd-skipped family developmental regulators. The Osr1 protein contains three zinc-finger motifs whereas Osr2 exists in two isoforms, containing three and five zinc-finger motifs respectively, due to alternative splicing of the transcripts. Targeted null mutations in these genes in mice resulted in distinct phenotypes, with heart and urogenital developmental defects in *Osr1*$^{-/-}$ mice and with cleft palate and open eyelids at birth in *Osr2*$^{-/-}$ mice. To investigate whether these contrasting mutant phenotypes are due to differences in their protein structure or to differential expression patterns, we generated mice in which the endogenous *Osr2* coding region was replaced by either *Osr1* cDNA or *Osr2A* cDNA encoding the five-finger isoform. The knockin alleles recapitulated endogenous *Osr2* mRNA expression patterns in most tissues and completely rescued cleft palate and cranial skeletal developmental defects of *Osr2*$^{-/-}$ mice. Mice hemizygous or homozygous for either knockin allele exhibited open-eyelids at birth, which correlated with differences in expression patterns between the knockin allele and the endogenous *Osr2* gene during eyelid development. Molecular marker analyses in *Osr2*$^{-/-}$ and *Osr2*$^{Osr1ki/Osr1ki}$ mice revealed that Osr2 controls eyelid development through regulation of the Fgf10–Fgfr2 signaling pathway and that Osr1 rescued Osr2 function in maintaining *Fgf10* expression during eyelid development in *Osr2*$^{Osr1ki/Osr1ki}$ mice. These results indicate that the distinct functions of Osr1 and Osr2 during mouse development result from evolutionary divergence of their *cis* regulatory sequences rather than distinct biochemical activities of their protein products.

Introduction

The *odd-skipped* (*odd*) gene was first identified in a large mutagenesis screen for developmental control genes in *Drosophila* (Nusslein-Volhard and Wieschaus, 1980). In the trunk of *odd* mutant embryos, cuticular defects appear limited to alternate, odd-numbered segments, hence the gene name and its designation as a pair-rule gene (Nusslein-Volhard and Wieschaus, 1980). Molecular cloning of the *odd* locus showed that it encodes a protein containing four contiguous C2H2-type zinc finger repeats (Coulter et al., 1990). By screening a *Drosophila* embryonic cDNA library using an *odd* DNA probe, Hart et al. (1996) identified two *odd*-cognate genes, *brother of odd with entrails limited* (*bowl*) and *sister of odd and bowl* (*sob*), which each encodes a protein with five highly conserved C2H2-type zinc finger tandem repeats. The fourth member of the *odd-skipped* gene family in *Drosophila*, *drumstick* (*drm*), was identified during characterization of genes regulating embryonic hindgut elongation (Green et al., 2002). In contrast to *odd*, *bowel*, and *sob*, *drm* encodes a small protein containing only two zinc finger motifs, of which only the first finger conforms to the canonical C2H2 sequence and shows high sequence identity to the first zinc finger in the other three Odd-skipped family proteins (Green et al., 2002).

The *odd*, *sob*, and *drm* genes are clustered together on the second chromosome and exhibit near identical patterns, but different levels, of expression during *Drosophila* embryogenesis, suggesting that they may function partially redundantly (Hart et al., 1996; Green et al., 2002; Johansen et al., 2003). Indeed, extensive mutagenesis screens have failed to recover a mutation in *sob* with any embryonic developmental defect (Johansen et al., 2003). Although ODD and DRM proteins have limited amino acid sequence identity, ectopic expression of *odd* and *drm* in the same tissues often resulted in similar developmental defects (Green et al., 2002; Hao et al., 2003; de Celis Ibeas and Bray, 2003; Hatini et al., 2005; Bras-Pereira et al., 2006). However, *odd* is required for embryonic segmentation whereas mutations in *drm* disrupted hindgut and proventriculus morphogenesis without affecting segmentation (Nusslein-Volhard and Wieschaus, 1980; Coulter and Wieschaus, 1988; Green et al., 2002).

Bowl, on the other hand, is expressed in a largely distinct pattern and exhibits clearly distinct functions from the other *odd-skipped* family genes during embryogenesis and tissue morphogenesis (Hart et al., 1996; Wang and Coulter, 1996; Hao et al., 2003; Johansen et al., 2003). Although *bowl* and *odd* have partially overlapping expression

* Corresponding author. Center for Oral Biology, University of Rochester, 601 Elmwood Avenue, Box 611, Rochester, NY 14642, USA. Fax: +1 585276 0190.
E-mail address: Rulang_Jiang@urmc.rochester.edu (R. Jiang).

0012-1606/$ – see front matter © 2009 Elsevier Inc. All rights reserved.
doi:10.1016/j.ydbio.2009.01.008

domains during embryogenesis and *bowl* mutants occasionally exhibited a mild segmentation defect, their mutant phenotypes are distinct from each other and *odd*/*bowl* double mutants did not show any synergism (Wang and Coulter, 1996). Moreover, whereas *bowl* and *drm* mutants exhibit similar defects in proventriculus and hindgut morphogenesis, *bowl drm odd* and *sob* compound mutants had no additional defects in gut development even though both *odd* and *sob* are co-expressed with *drm* and the domains of their expression also partially overlap with that of *bowl* during gut development (Johansen et al., 2003). Furthermore, although there is significantly more extensive amino acid sequence identity between ODD and BOWL than that between ODD and DRM proteins, ectopic expression of *bowl* almost always resulted in different phenotypes from that of ectopic expression of *odd* or *drm* under the same conditions (Hao et al., 2003; Bras-Pereira et al., 2006). For example, ectopic expression of *drm* throughout the developing hindgut caused dramatic expansion of the small intestine whereas ectopic expression of *bowl* using the same driver had little effect on the morphology and patterning of the gut (Johansen et al., 2003). Together, these data indicate that the protein products of *odd* and its cognate genes have largely distinct functions during *Drosophila* development.

In the mammalian genome, only two *odd-skipped* related genes, *Osr1* and *Osr2*, exist. *Osr1* encodes a protein with three zinc fingers and *Osr2* encodes both a three-finger (Osr2B) and a five-finger (Osr2A) protein due to alternative splicing of the pre-mRNA (So and Danielian, 1999; Lan et al., 2001; Katoh, 2002; Kawai et al., 2005). While their structural homology to the *Drosophila* ODD family proteins is limited to the zinc finger motifs, Osr1 and Osr2B show 65% amino acid sequence identity overall and 98% amino acid sequence identity in their zinc finger domains (Lan et al., 2001). During mouse embryonic development and organogenesis, *Osr1* and *Osr2* exhibit distinct as well as partially overlapping expression patterns (So and Danielian, 1999; Lan et al., 2001, 2004; Stricker et al., 2006). Targeted null mutations in *Osr1* and *Osr2* in mice resulted in distinct phenotypes, with heart and urogenital developmental defects in $Osr1^{-/-}$ mice and with cleft palate and open-eyelids at birth in $Osr2^{-/-}$ mice (Lan et al., 2004; Wang et al., 2005; James et al., 2006). Whereas the early embryonic lethality of $Osr1^{-/-}$ mutant mice precluded direct analysis of the roles of *Osr1* in many developmental processes in those mutants, the correlation of developmental defects in the $Osr2^{-/-}$ mutants to specific tissues that normally do not express *Osr1* and the lack of phenotypes in $Osr2^{-/-}$ mutants in many tissues where *Osr1* and *Osr2* are normally co-expressed suggest that *Osr1* and *Osr2* function partly redundantly during mouse embryonic development (Lan et al., 2004; Wang et al., 2005). However, Kawai et al. (2005) reported that the two Osr2 isoforms, containing three (Osr2B) and five (Osr2A) zinc finger repeats respectively, when fused to the Gal4 DNA binding domain, exhibited opposite transcriptional activity in a cell culture based reporter assay. Since the *Osr1* gene product only contains three zinc-finger repeats, it is possible that Osr1 and Osr2B may have similar biochemical functions due to their overall amino acid sequence homology whereas Osr2A may have evolved distinct functions. To directly address whether the mammalian Osr1 and the two Osr2 isoforms have evolved distinct biochemical functions *in vivo*, we have generated mice with the *Osr2* gene coding region replaced by either an *Osr1* cDNA or an *Osr2A* cDNA through targeted gene replacement in mice. Here we show that these two gene substitution strategies similarly rescued the developmental defects of the $Osr2^{-/-}$ mutant mice.

Materials and methods

Generation of mice carrying $Osr2^{Osr1ki}$ and $Osr2^{Osr2Aki}$ alleles

A 129/SvEv strain mouse BAC clone containing the entire *Osr2* genomic region, as reported previously (Lan et al., 2004), was used for gene targeting vector construction. To replace the Osr2 coding region with either *Osr1* cDNA or *Osr2A* cDNA, a 2 kb genomic fragment immediately 5′ to the translation start codon (ATG) of the *Osr2* gene was amplified by PCR, subcloned, sequenced, and used as the 5′ homology arm of the targeting vectors. A hexameric Myc epitope-tag coding region from the pCS+MT vector (Rupp et al., 1994) was ligated in-frame to the 5′ end of PCR-amplified cDNA fragments containing either *Osr1* or *Osr2A* coding sequences, each ending 3′ to their respective translation stop codon. The targeting vectors contain the 2 kb 5′ homology arm described above, either the *Myc-Osr1* or the *Myc-Osr2A* cDNA cassette, followed by a loxP-flanked *PGK-neo* expression cassette for positive selection, a 3.3 kb 3′ homology arm containing the 3′ untranslated region of the *Osr2* gene, and a *PGK-DTA* expression cassette for negative selection (Fig. 1). Correct targeting of the *Osr2* locus results in deletion and replacement of the 2.6 kb region from the translation start codon in Exon 2 through the middle of the 3′ untranslated region in Exon 4 with the *Myc-Osr1* or *Myc-Osr2A* cDNA, and the *neo* expression cassette (Fig. 1).

The targeting vectors were linearized and electroporated into CJ7 ES cells. ES cell culture and Southern screening of ES clones were carried out as previously described (Swiatek and Gridley, 1993; Lan et al., 2004). Two independent correctly targeted ES cell clones for each of the targeting vectors were injected into blastocysts from C57BL/6J mice and the chimeric male mice were bred with C57BL/6J females to test for germline transmission. Tail DNA of F1 mice were used for genotyping by PCR and Southern hybridization. Mice and embryos from subsequent generations were genotyped by PCR. PCR with primer 1 (5′-GAT ACG GGT AAG ACA GAA ACT G-3′) and primer 2 (5′-CTA CAA GGA TCT AGC ACA TGC TG-3′) amplifies a 490 bp band from the wild-type *Osr2* allele. PCR with primer 2 and primer 3 (5′-CTT CTT GAC GAG TTC TTC TGA GG-3′) amplifies a 460 bp allele-specific product from either the $Osr2^{Osr1ki}$ or the $Osr2^{Osr2Aki}$ allele. Heterozygous F1 mice were either crossed with the $Osr2^{+/-}$ mice (heterozygous for the $Osr2^{tm1Jian}$ allele, Lan et al., 2004) to generate $Osr2^{Osr1ki/-}$ and $Osr2^{Osr2Aki/-}$ hemizygous mice or intercrossed to generate $Osr2^{Osr1ki/Osr1ki}$ and $Osr2^{Osr2Aki/Osr2Aki}$ homozygous knockin mice, respectively.

Skeletal analysis, histology and in situ hybridization

Skeletal preparations of newborn mice were carried out following the protocol described by Martin et al. (1995). For histology and in situ hybridization, embryos were dissected at desired developmental stages. Tail DNA or yolk sac DNA was extracted and genotypes of the embryos were determined by allele-specific PCR. For histology analysis, embryos were fixed in Bouin's fixative, then dehydrated through graded ethyl alcohols, embedded in paraffin, sectioned at 7 μm thickness and stained with hematoxylin and eosin. For in situ hybridization, embryos were fixed in 4% paraformaldehyde in PBS overnight at 4 °C. Sectioned in situ hybridization was carried out as previously described (Lan et al., 2001) with digoxygenin-labeled antisense RNA probes.

Detection of cell proliferation

For detection of cell proliferation in the developing eyelids, timed pregnant female mice were injected intraperitoneally on gestational day 13.5 with BrdU (Roche) labeling reagent (45 μg/g body weight). One hour after injection, embryos were dissected, fixed in Carnoy's fixative, dehydrated through graded alcohols, embedded in paraffin and sectioned in the coronal plane at 5 mm thickness. Immunodetection of BrdU was performed using the BrdU labeling and detection kit (Roche) according to manufacturer's instructions and the sections were counterstained with nuclear fast red to visualize all cellular nuclei. The total number of cell nuclei as well as the number of BrdU-

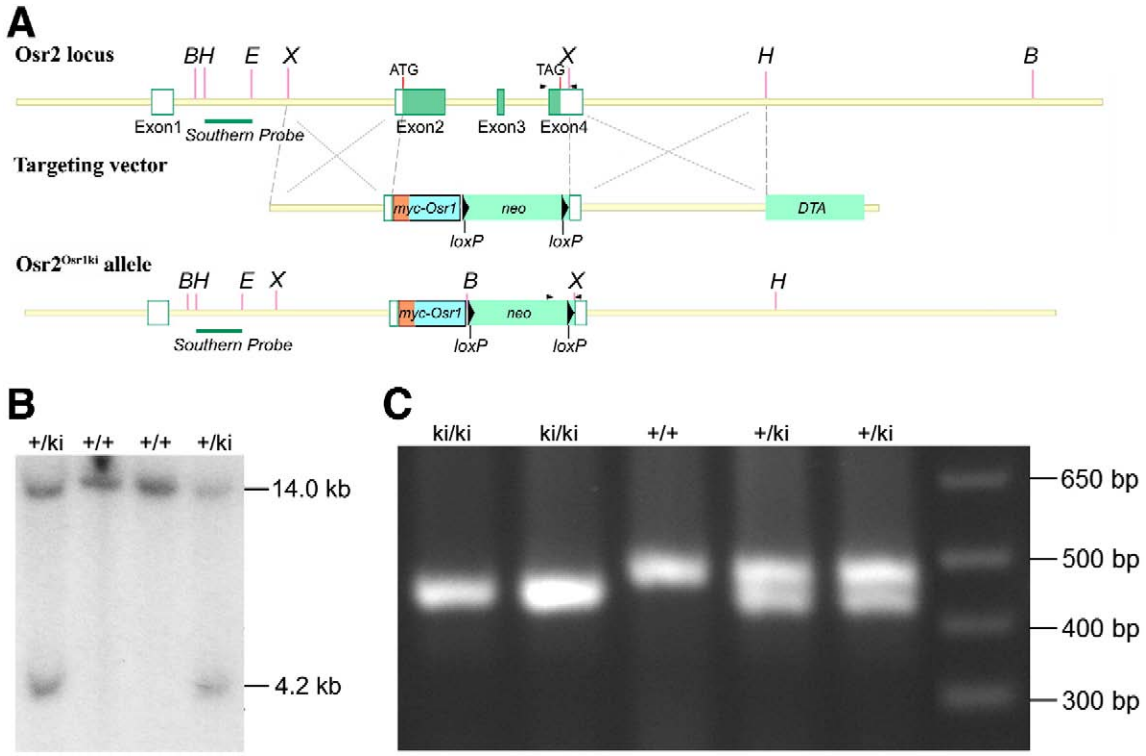

Fig. 1. Targeted replacement of the mouse *Osr2* gene coding region with *Myc-Osr1* cDNA. (A) The *Osr2* gene contains four exons that span approximately 8 kb of genomic DNA. Exons are shown as boxes, with the protein-coding region marked in green. The positions of the translation start (ATG) and stop (TAG) codons are indicated. The targeting vector used the 2 kb fragment containing the intron 1/exon 2 junction as the 5′ homology arm and the 3.3 kb XbaI–HindIII fragment 3′ to the coding region as the 3′ arm. The *Myc-Osr1* cDNA and a loxP-flanked *neo* expression cassette were inserted in between the arms and a diphtheria toxin A (*DTA*) expression cassette was cloned 3′ to the 3′ arm for negative selection against random integration. Arrowheads above the wild-type and $Osr2^{Osr1ki}$ genomic schematics indicate the positions of PCR primers used for genotyping. (B) Southern hybridization analysis of ES cell clones showing correct targeting of the *Osr2* locus. The 14 kb BamHI fragment corresponding to the wild-type allele was detected in all ES cell clones, while the 4.2 kb *Osr1*-knockin allele-specific fragment was detected only in ES cell clones heterozygous for the knockin allele. (C) PCR analysis of tail DNA samples from newborn F2 progeny. The fragments amplified from wild-type and knockin alleles are 490 bp and 460 bp, respectively. +/+, wild-type; +/ki, heterozygote; ki/ki, homozygote.

labeled nuclei on sections through the middle of the upper and lower eyelids were counted and recorded separately for the epithelium and mesenchyme from ten continuous sections. The cell proliferation index was calculated as percentage of the cell nuclei with BrdU labeling. Students' *t*-test was used to analyze the significance of difference and a *P* value less than 0.05 was considered statistically significant.

Results

Generation of $Osr2^{Osr1ki/-}$ and $Osr2^{Osr1ki/Osr1ki}$ mice

To directly analyze whether Osr1 and Osr2 have equivalent or distinct functions *in vivo*, we used the gene targeting technology to replace the *Osr2* coding region with a *Myc-Osr1* cDNA together with a loxP-flanked *neo* expression cassette (Fig. 1A). Chimeric mice were generated from two correctly targeted ES cell clones and germ line transmission of the targeted allele was confirmed with Southern hybridization of F1 mouse progeny tail DNA samples (Fig. 1B). F1 mice heterozygous for the $Osr2^{Osr1ki}$ allele were indistinguishable phenotypically from wild-type mice and were fertile. $Osr2^{Osr1ki/+}$ heterozygotes were either crossed with $Osr2^{+/-}$ heterozygous mice to generate $Osr2^{Osr1ki/-}$ hemizygotes or intercrossed to generate $Osr2^{Osr1ki/Osr1ki}$ mice.

Since a similarly targeted $Osr2^{tm1Jian}$ allele, in which the *Osr2* gene was deleted from the middle of Exon 2 to the 3′ untranslated region in Exon 4 and replaced by an in-frame fusion of the *lacZ* reporter gene, resulted in LacZ expression recapitulating endogenous *Osr2* expression patterns during early mouse embryogenesis (Lan et al., 2004), we expected that the $Osr2^{Osr1ki}$ allele will result in expression of *Myc-Osr1* in the same pattern as endogenous *Osr2* mRNA expression. To test this, we compared *Osr1* and *Osr2* mRNA expression at selected stages of palate development by in situ hybridization analysis. As reported previously (Lan et al., 2001, 2004), *Osr2* mRNA is expressed in a lateral–medial gradient, with lower levels in the medial side, in the developing palatal shelves at E13.5 in wild-type embryos (Fig. 2A). In contrast, *Osr1* mRNA is weakly expressed only in the lateral half, but not in the medial half, of the developing palatal mesenchyme at this stage (Fig. 2D). Both *Osr1* and *Osr2* mRNAs are expressed in the mandibular mesenchyme lateral to the developing molar tooth buds (Figs. 2A, D). In addition, whereas *Osr2* mRNA is strongly expressed in the maxillary and mandibular mesenchyme on the lingual side of the molar tooth buds (Fig. 2A), *Osr1* is only weakly expressed in a subset of mesenchymal cells lingual to the mandibular tooth bud but not in the maxillary molar tooth mesenchyme (Fig. 2D). Consistent with the differential expression of *Osr1* and *Osr2* in the developing tooth mesenchyme, we recently discovered that Osr2 antagonizes the Msx1-Bmp4 molecular pathway to pattern the buccolingual axis of the molar tooth developmental field and that $Osr2^{-/-}$ mutant mice exhibit supernumerary tooth formation lingual to the normal molar teeth (Zhang et al., submitted, and Fig. 3B). No *Osr2* mRNA expression was detected in all tissues and developmental stages examined in the $Osr2^{Osr1ki/-}$ hemizygous and $Osr2^{Osr1ki/Osr1ki}$ homozygous embryos (Figs. 2B, C, and data not shown), consistent with deletion of the coding region of the endogenous *Osr2* gene in these embryos. *Osr1* mRNA expression, in contrast, is clearly detected in the $Osr2^{Osr1ki/-}$ hemizygous and $Osr2^{Osr1ki/Osr1ki}$ homozygous embryos in the tissues

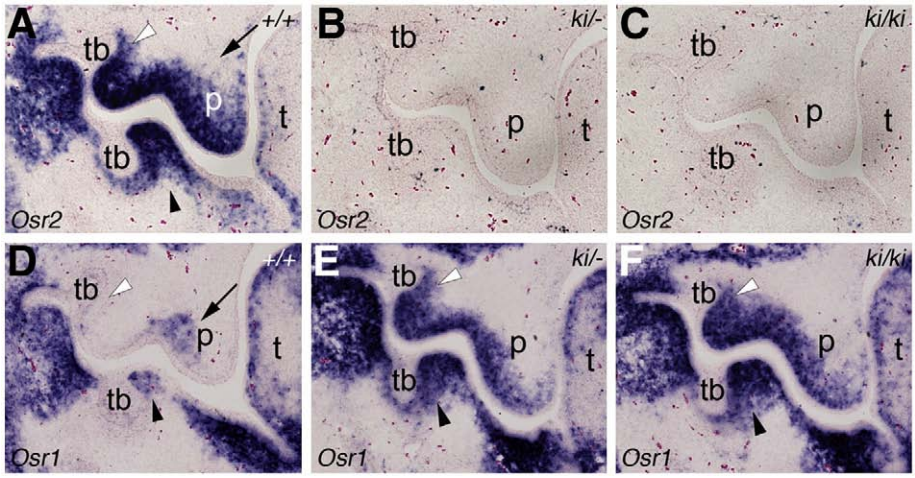

Fig. 2. Comparison of *Osr1* and *Osr2* expression patterns in wild-type, $Osr2^{Osr1ki/-}$ and $Osr2^{Osr1ki/Osr1ki}$ embryos. mRNA signals are shown in dark blue in all panels. (A) At E13.5, *Osr2* mRNA is abundantly expressed in palatal shelves (arrow) and in the mesenchyme lingual to the developing molar tooth buds (arrowheads). In E13.5 $Osr2^{Osr1ki/-}$ and $Osr2^{Osr1ki/Osr1ki}$ embryos (B and C), no *Osr2* expression was detected. (D) At E13.5, the lateral halves of the palatal shelves express moderate levels of *Osr1* mRNA (arrow), while the medial halves of the palatal shelves completely lack *Osr1* mRNA expression. A few cells in the mesenchyme lingual to the mandibular molar tooth buds express *Osr1* mRNA (arrowhead). Abundant expression of *Osr1* at E13.5 was detected in the developing tongue and lateral regions of the mandible. (E, F) In E13.5 $Osr2^{Osr1ki/-}$ and $Osr2^{Osr1ki/Osr1ki}$ embryos, *Osr1* is expressed in its endogenous expression domains as well as in regions where only *Osr2* is expressed in wild-type embryos, including the medial sides of the palatal shelves and the mesenchyme lingual to the developing maxillary and mandibular molar tooth buds (arrowheads). p, palate shelf; t, tongue; tb, tooth bud. Embryo genotypes marked on the upper right corner of each panel are: +/+, wild-type; *ki*/—, $Osr2^{Osr1ki/-}$ hemizygous; *ki*/*ki*, $Osr2^{Osr1ki/Osr1ki}$ homozygous.

that normally express *Osr2* but not *Osr1* mRNA, including the medial side of the developing palatal shelves and in the lingual side of the developing molar tooth mesenchyme (Figs. 2E, F). Thus, the *Osr2*-allele drives *Osr1* mRNA expression under the control of the *Osr2 cis* regulatory sequences and makes it possible to directly test whether Osr1 and Osr2 are functionally equivalent *in vivo*.

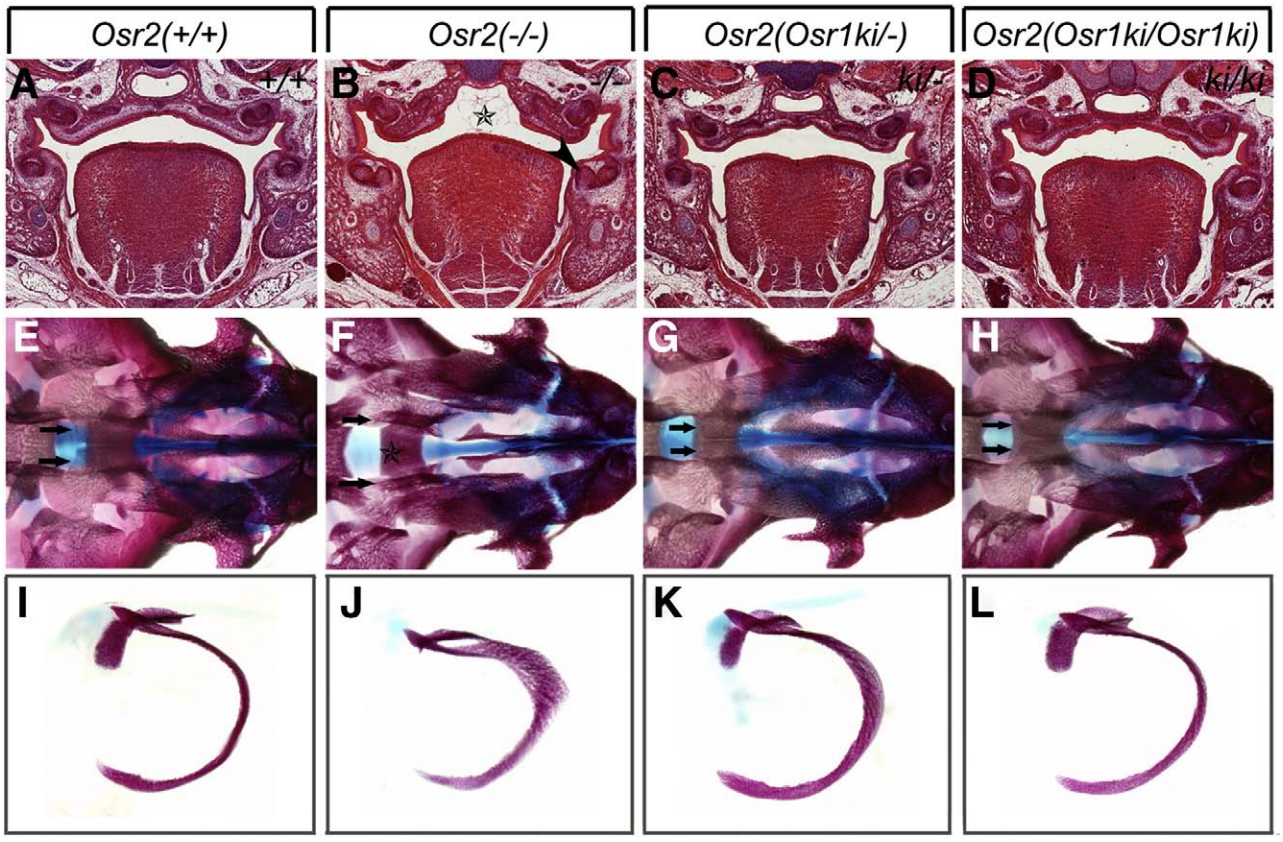

Fig. 3. Expression of *Myc-Osr1* from the *Osr2* locus rescues cleft palate, tooth and tympanic ring abnormalities of $Osr2^{-/-}$ mutant mice. (A, B) $Osr2^{-/-}$ mutant mice exhibit bilateral cleft palate (star in panel B) and supernumerary teeth lingual to the molars (arrowhead in panel B), in comparison to the wild-type littermate (A). (C, D) Both $Osr2^{Osr1ki/-}$ (C) and $Osr2^{Osr1ki/Osr1ki}$ (D) mice exhibit normal palate and tooth development. (E–H) Skeletal preparations showing palatine bone defects in the $Osr2^{-/-}$ mutants (F) and normal palatine bone in wild-type (E), $Osr2^{Osr1ki/-}$ (G) and $Osr2^{Osr1ki/Osr1ki}$ (H) newborn mice. Arrows in panels E–H point to the palatine bones. The star in F marks the presphenoid bone, which is normally covered under the palatine bones from the oral view of the cranial skeleton (such as in panels E, G, H) but completely exposed in the $Osr2^{-/-}$ mutant skeleton due to cleft palate. (I–L) $Osr2^{-/-}$ mutants have significantly reduced and thickened tympanic rings (J) as compared with the wild-type control (I). The tympanic rings of the $Osr2^{Osr1ki/-}$ (K) and $Osr2^{Osr1ki/Osr1ki}$ (L) mice are comparable in size to the wild-type controls.

Expression of Osr1 from the Osr2 locus completely rescues the cleft palate, supernumerary tooth, and tympanic ring phenotypes of the $Osr2^{-/-}$ mutant mice

$Osr2^{Osr1ki/+}$ mice were crossed with $Osr2^{+/-}$ mice or intercrossed to generate $Osr2^{Osr1ki/-}$ hemizygous and $Osr2^{Osr1ki/Osr1ki}$ mice, respectively. The $Osr2^{Osr1ki/-}$ hemizygous and $Osr2^{Osr1ki/Osr1ki}$ homozygous mice were born at expected Mendelian ratios and both genotypes survived postnatally, exhibited similar life span to wild-type and heterozygous mice and were fertile. Litter size from either intercrosses of these genotypes or outcrosses to wild-type mice was similar to wild-type mice in the same genetic background. Detailed histological analysis of $Osr2^{Osr1ki/-}$ and $Osr2^{Osr1ki/Osr1ki}$ fetal mice showed that palate development occurred normally in these mice, indicating that the *Myc-Osr1* expressed from the *Osr2* locus rescued the cleft palate defect of $Osr2^{-/-}$ mutant mice (Figs. 3A–D). Similarly, tooth development appeared normal in the $Osr2^{Osr1ki/-}$ hemizygous and $Osr2^{Osr1ki/Osr1ki}$ homozygous mice (Fig. 3D, and data not shown). In addition, examination of skeletal preparations of newborn mice did not detect any skeletal abnormalities in comparison with wild-type and heterozygous littermates. Specifically, while the $Osr2^{-/-}$ mutant pups had defects in palatine bones, the $Osr2^{Osr1ki/-}$ hemizygous and $Osr2^{Osr1ki/Osr1ki}$ homozygous mice all had similar palatine bones to the wild-type littermates (Figs. 3E–H). In addition, while the tympanic rings of newborn $Osr2^{-/-}$ mutant mice were thickened and significantly reduced in size, in comparison with wild-type littermates (Lan et al., 2004, Figs. 3I, J), the tympanic rings of newborn $Osr2^{Osr1ki/-}$ hemizygous and $Osr2^{Osr1ki/Osr1ki}$ homozygous mice were normal in size although they were still slightly thickened in the $Osr2^{Osr1ki/-}$ hemizygous mice (Figs. 3K, L). These data indicate that *Osr1*, when expressed under the control of the regulatory sequences of *Osr2* locus, can carry out all the essential functions of *Osr2* during palate, tooth, and tympanic ring development.

$Osr2^{Osr1ki/-}$ hemizygous and $Osr2^{Osr1ki/Osr1ki}$ homozygous mice exhibit open-eyelids at birth due to subtle differences in the expression patterns of $Osr2^{Osr1ki}$ and endogenous Osr2 alleles

As reported previously (Lan et al., 2004), $Osr2^{-/-}$ mutant mice are born with open eyelids (Fig. 4B). We found that $Osr2^{Osr1ki/-}$ hemizygous mice are born with an open eyelid defect similar to that of the $Osr2^{-/-}$ mutants (Fig. 4C). The severity of the open eyelid defect is greatly reduced in $Osr2^{Osr1ki/Osr1ki}$ mice, however, it is still identifiable as a small opening in the middle part of the eyelids at birth (Fig. 4D). Since the $Osr2^{Osr1ki}$ allele contains a loxP-flanked *PGK-neo* expression cassette, which has been shown to interfere with gene expression in some gene-targeted mouse strains (Olson et al., 1996; Seidl et al., 1999; Holzenberger et al. 2000), it is possible that the open eyelid defect in the $Osr2^{Osr1ki/-}$ and $Osr2^{Osr1ki/Osr1ki}$ mice might result from interference of *Myc-Osr1* expression by the *PGK-neo* cassette. To test this possibility, $Osr2^{Osr1ki/+}$ heterozygous mice were crossed to *EIIa-Cre* transgenic mice (Lakso et al., 1996) to delete the *PGK-neo* expression cassette from the targeted *Osr2* locus. $Osr2^{Osr1ki/+}$*EIIa-Cre* double heterozygous mice were crossed to $Osr2^{+/-}$ mice or intercrossed to generate $Osr2^{Osr1ki/-}$*EIIa-Cre* mice and $Osr2^{Osr1ki/Osr1ki}$*EIIa-Cre* mice, respectively. Southern hybridization and PCR analyses of tail genomic DNA samples confirmed that the *PGK-neo* cassette had been deleted from the targeted *Osr2* locus in these mice (data not shown). However, they were still born with an open eyelid phenotype with severity similar to the $Osr2^{Osr1ki/-}$ hemizygous and $Osr2^{Osr1ki/Osr1ki}$ homozygous mice, respectively (data not shown).

Another possible reason why the $Osr2^{Osr1ki/-}$ and $Osr2^{Osr1ki/Osr1ki}$ mice are born with open eyelids is that the $Osr2^{Osr1ki}$ allele may have failed to completely recapitulate the endogenous *Osr2* gene expression pattern during eyelid development. Thus, we compared the expression patterns of *Osr1* mRNA in the developing eyelid regions in wild-type and $Osr2^{Osr1ki/Osr1ki}$ embryos with that of *Osr2* mRNA in wild-type embryos. In wild-type embryos at E13.5, *Osr2* mRNA was strongly expressed in both the epithelium and mesenchyme of developing eyelids (Fig. 5A). In contrast, endogenous *Osr1* mRNA expression was only expressed in a small subset of mesenchymal cells at the base of the eyelids at this stage (Fig. 5B). In the $Osr2^{Osr1ki/Osr1ki}$ homozygous embryos at E13.5, *Osr1* mRNA was moderately expressed in the developing eyelid mesenchyme but expression in the eyelid epithelium was much weaker (Fig. 5C), in contrast to the strong *Osr2* mRNA expression in the same areas of the developing eyelids in the wild-type embryos (Fig. 5A). To investigate whether the differences in the expression patterns between $Osr2^{Osr1ki}$ allele and the endogenous *Osr2* gene were due to deletion of *Osr2* gene sequences in the knockin allele, we analyzed *lacZ* expression from the previously targeted $Osr2^{tm1Jian}$ allele, which carries deletion of the same genomic region containing the second and third introns, in $Osr2^{+/-}$ mice. As shown in Fig. 5D, *lacZ* expression in the developing eyelids in $Osr2^{+/-}$ mice is also much weaker in the epithelium than in the mesenchyme. These data suggest that the open-eyelids phenotype in the $Osr2^{Osr1ki/-}$ hemizygous and $Osr2^{Osr1ki/Osr1ki}$ homozygous mice resulted from deletion of *cis* regulatory sequences in the *Osr2* gene necessary for complete recapitulation of the endogenous *Osr2* gene expression pattern by the $Osr2^{Osr1ki}$ allele.

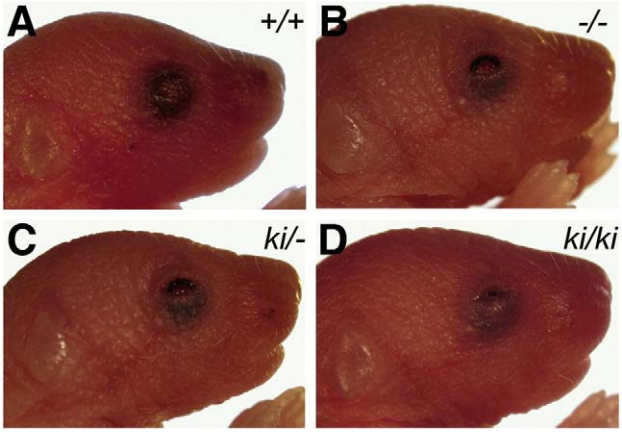

Fig. 4. The $Osr2^{Osr1ki/-}$ and $Osr2^{Osr1ki/Osr1ki}$ mice were born with open eyelids. $Osr2^{Osr1ki/-}$ mice (C) are born with open eyelid defect with a similar severity as that of the $Osr2^{-/-}$ mutants (B). The severity of the open eyelid defect is greatly reduced in $Osr2^{Osr1ki/Osr1ki}$ mice (D), however it is still identifiable as a small opening in the middle part of the eyelids. +/+, wild-type; −/−, $Osr2^{-/-}$ homozygote; *ki*/−, $Osr2^{Osr1ki/-}$ hemizygote; *ki*/*ki*, $Osr2^{Osr1ki/Osr1ki}$ homozygote.

Comparison of functions of the three-finger Osr1 protein with that of the five-finger Osr2A protein isoform in vivo

The *Osr2* gene encodes two mRNA isoforms, *Osr2A* and *Osr2B*, differing by the presence or absence of an 82-nucleotide sequence corresponding to the beginning of the fourth exon, due to alternative splicing (Kawai et al., 2005). Whereas *Osr2A* encodes a protein containing five contiguous zinc finger repeats, homologous to the *Drosophila* BOWL and SOB proteins, the 82-nucleotide deletion in *Osr2B* results in a frame shift and an in-frame translation stop codon shortly after the third zinc finger-coding region. Kawai et al. (2005) reported that Osr2A and Osr2B exhibited opposite transcriptional activity when fused with the Gal4 DNA-binding domain and co-transfected into COS-7 cells with a luciferase reporter under the control of five tandem Gal4 binding sites. Since the mouse Osr1 and Osr2B proteins both contain only three zinc finger motifs and they share 65% identity in overall amino acid sequences and 98% identity in the three zinc finger motifs (Lan et al., 2001), it is possible that the

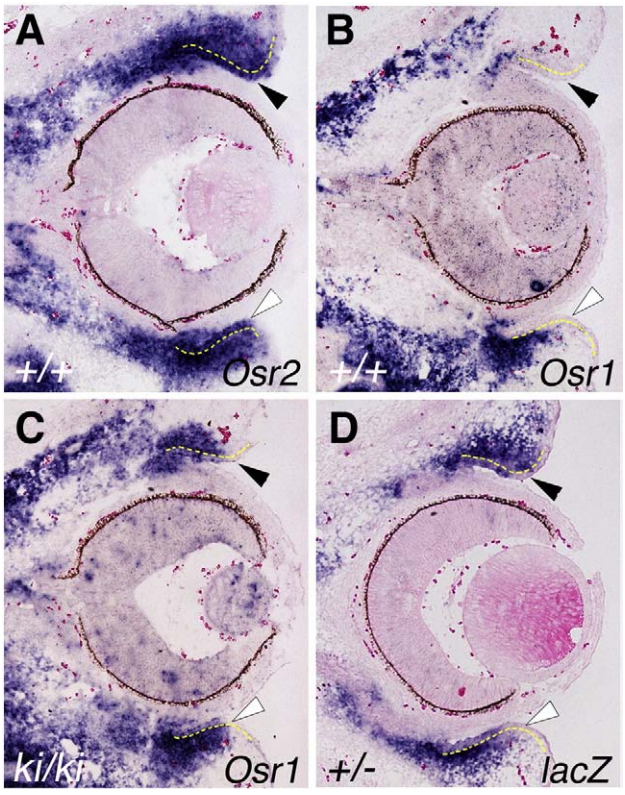

Fig. 5. Expression of *Myc-Osr1* in the $Osr2^{Osr1ki/Osr1ki}$ embryos did not completely recapitulate endogenous *Osr2* expression pattern during eyelid development. (A, B) At E13.5, *Osr2* mRNA is strongly expressed throughout the developing upper and lower eyelid tissues in the wild-type mouse embryo (A) while *Osr1* mRNA is only expressed in the proximal region of the lower eyelid and undetectable in the developing upper eyelid (B). (C) In $Osr2^{Osr1ki/Osr1ki}$ embryos at E13.5, *Osr1* mRNA is expressed in both the upper and lower eyelids. In contrast to the *Osr2* expression pattern in wild-type embryos, *Osr1* expression in the developing eyelid epithelium is much weaker than that in the mesenchyme in the $Osr2^{Osr1ki/Osr1ki}$ embryos. Black arrowheads point to the upper eyelid epithelium, while white arrowheads point to the lower eyelid epithelium in all panels. Yellow dashed lines mark the eyelid epithelium-mesenchyme boundary. (D) *lacZ* mRNA in the $Osr2^{tm1Jian}$ heterozygous embryos also showed much weaker expression in the epithelium than in the mesenchyme of the developing eyelids at E13.5. +/+, wild-type; +/−, $Osr2^{tm1Jian}$ heterozygote; *ki*/*ki*, $Osr2^{Osr1ki/Osr1ki}$ homozygote.

Myc-Osr1 expressed from the $Osr2^{Osr1ki}$ allele could only replace the function of the Osr2B isoform but not that of the five-finger Osr2A isoform, which may be part of the reason why expression of *Myc-Osr1* from the $Osr2^{Osr1ki}$ allele failed to completely rescue the eyelid developmental defects of $Osr2^{-/-}$ mutant mice. To test this possibility, we replaced the endogenous *Osr2* coding region with the *Osr2A* cDNA and a loxP-flanked *PGK-neo* expression cassette using a gene targeting vector essentially the same as the $Osr2^{Osr1ki}$ targeting vector but using *Myc-Osr2A* cDNA in place of the *Myc-Osr1*

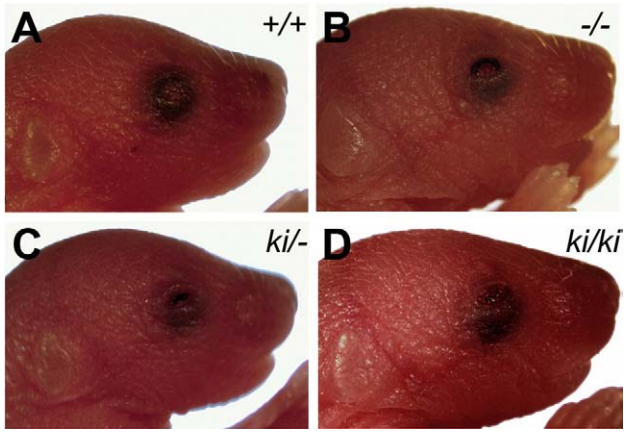

Fig. 6. The $Osr2^{Os2Aki/-}$ and $Osr2^{Osr2Aki/Osr2Aki}$ mice were also born with an open eyelid phenotype. Compared with the $Osr2^{-/-}$ mice, the severity of the open eyelid defect is greatly reduced in the $Osr2^{Os2Aki/-}$ (C) and $Osr2^{Osr2Aki/Osr2Aki}$ mice (D). +/+, wild-type; −/−, $Osr2^{-/-}$ homozygote; *ki*/−, $Osr2^{Osr2Aki/-}$ hemizygote; *ki*/*ki*, $Osr2^{Osr2Aki/Osr2Aki}$ homozygote.

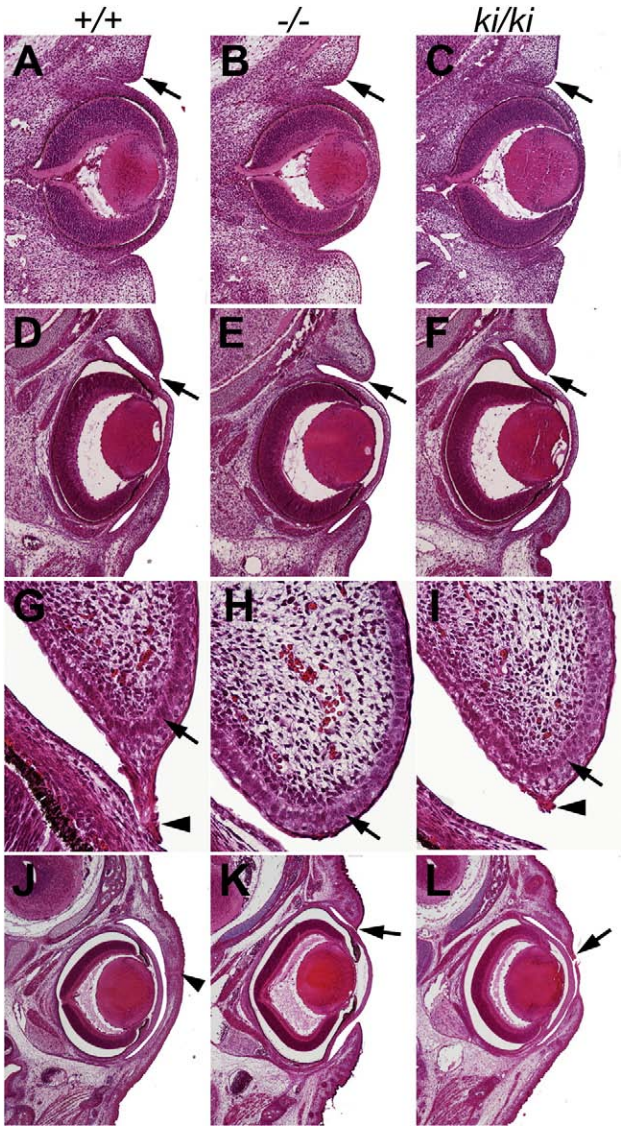

Fig. 7. Histological analysis of eyelid development in wild-type, $Osr2^{-/-}$ and $Osr2^{Osr1ki/Osr1ki}$ mice. (A–C) Frontal sections through the middle of the developing eye in E13.5 wild-type (A), $Osr2^{-/-}$ (B) and $Osr2^{Osr1ki/Osr1ki}$ (C) embryos. Arrows in panels A–C point to the upper eyelid primordia. (D–F) Frontal sections through the middle of the developing eye in E14.5 wild-type (D), $Osr2^{-/-}$ (E) and $Osr2^{Osr1ki/Osr1ki}$ (F) embryos. Arrows point to the leading edge of the developing upper eyelids. (G–I) High magnification views of the leading edges of the developing upper eyelids in E14.5 wild-type (G), $Osr2^{-/-}$ (H) and $Osr2^{Osr1ki/Osr1ki}$ (I) embryos. Arrows point to the basal layer of the epithelium, which has spindle-shaped nuclei in wild-type (G) and round nuclei in the $Osr2^{-/-}$ mutant (H) eyelids. The nuclei of the basal layer epithelium in the $Osr2^{Osr1ki/Osr1ki}$ (I) eyelids appear rounder than those in the wild-type eyelids but better organized than those in $Osr2^{-/-}$ mutant eyelid. Arrowheads in panels G and I point to the leading edge periderm cells. (J) Frontal section through the middle of a wild-type E16.5 embryo eye. The eyelids have completed fusion. Arrowhead points to the fused epithelial seam. (K, L) Frontal sections through middle of the eyes in E18.5 $Osr2^{-/-}$ (K) and $Osr2^{Osr1ki/Osr1ki}$ (L) mice. The upper and lower eyelids are still separated widely in the $Osr2^{-/-}$ mutant (K) at E18.5, with only rudimentary epithelial ridge at the leading edge of the upper lid (arrow). In E18.5 $Osr2^{Osr1ki/Osr1ki}$ (L) mice, the leading edge periderm cells (arrow) migrated over the corneal surface but fusion between the upper and lower eyelids failed in the middle region of the eye, most likely due to the reduced size of the eyelids. +/+, wild-type; −/−, $Osr2^{-/-}$; *ki*/*ki*, $Osr2^{Osr1ki/Osr1ki}$ embryos.

cDNA (Fig. 1A). We obtained five correctly targeted ES clones and used two independent clones to generate chimeric mice. Chimeric males were crossed to C57BL/6J female mice and tail genomic DNA were analyzed by Southern hybridization and allele-specific PCR to confirm germline transmission of the targeted allele (data not shown). Mice heterozygous for the $Osr2^{Osr2Aki}$ allele are normal and fertile. $Osr2^{Osr2Aki/+}$ heterozygotes were crossed with $Osr2^{+/-}$ mice or intercrossed to generate $Osr2^{Osr2Aki/-}$ and $Osr2^{Osr2Aki/Osr2Aki}$ mice, respectively. The $Osr2^{Osr2Aki/-}$ and $Osr2^{Osr2Aki/Osr2Aki}$ mice were found at expected Mendelian ratios at weaning and exhibit comparable lifespan with wild-type littermates. Similar to the $Osr2^{Osr1ki}$ mice, $Osr2^{Osr2Aki/Osr2Aki}$ mice showed normal palate, tooth, and tympanic ring development (data not shown). Also similar to the $Osr2^{Osr1ki}$ mice, both $Osr2^{Osr2Aki/-}$ and $Osr2^{Osr2Aki/Osr2Aki}$ mice were born with open eyelids (Fig. 6), with the $Osr2^{Osr2Aki/Osr2Aki}$ homozygous mice displaying less severe open-eyelid defect than the $Osr2^{Osr2Aki/-}$ hemizygous mice. Thus, the $Osr2^{Osr2Aki/-}$ and $Osr2^{Osr2Aki/Osr2Aki}$ mice essentially phenocopy the $Osr2^{Osr1ki/-}$ and $Osr2^{Osr1ki/Osr1ki}$ mice, respectively. Furthermore, we crossed the $Osr2^{Osr1ki/Osr1ki}$ mice with $Osr2^{Osr2Aki/Osr2Aki}$ mice and generated $Osr2^{Osr1ki/Osr2Aki}$ transheterozygous mice, which were also born with a mild open-eyelid phenotype similar to either parent (data not shown). These data indicate that Osr1 and Osr2A display equivalent biochemical activities *in vivo* when expressed in the same cells, in spite of their differences in the number of zinc finger repeats.

Osr2 is required for eyelid growth and morphogenesis

Development of the eyelid requires coordinated growth, epithelial migration and fusion. In mice, eyelid outgrowth is initiated at E11.5, forming deep grooves above and below the developing optic vesicle by E13.5 (Tao et al., 2005). Compared with wild-type littermates, $Osr2^{-/-}$ mutant mice exhibited obvious retardation in eyelid outgrowth by E13.5 (Figs. 7A, B). In contrast, $Osr2^{Osr1ki/Osr1ki}$ embryos showed only slightly reduced eyelid primordial size compared with the wild-type embryos at this stage (Fig. 7C). By E15.5, both upper and lower eyelid epithelium formed leading edges that migrated toward each other over the surface of the developing cornea in wild-type embryos (Figs. 7D, G). The developing eyelids in $Osr2^{-/-}$ littermates at this stage appeared round and did not form the periderm leading edges seen in the wild-type littermates (Figs. 7E, H). The leading edges of the developing eyelids in $Osr2^{Osr1ki/Osr1ki}$ embryos at E15.5 formed rudimentary protruding periderm clumps but did not extend over the cornea (Figs. 7F, I). The wild-type eyelids had completed fusion by E16.5 (Fig. 7J), whereas the $Osr2^{-/-}$ mutant upper and lower eyelids were still separated wide apart at E18.5, although their leading edges started to form rudimentary epithelial ridges (Fig. 7K). By E18.5, the leading edge periderm cells of $Osr2^{Osr1ki/Osr1ki}$ upper and lower eyelids migrated over the developing cornea, but their eyelid bodies were too far apart to complete fusion over the central region of the cornea (Fig. 7L).

We performed BrdU incorporation assay to investigate the eyelid growth retardation phenotypes in $Osr2^{-/-}$ and $Osr2^{Osr1ki/Osr1ki}$ embryos. At E13.5, $Osr2^{-/-}$ mutant embryos showed about 50% reduction in cell proliferation in both upper and lower eyelid epithelium, compared to wild-type littermates (Figs. 8A–C). In addition, mesenchymal cell proliferation was also significantly reduced in both upper and lower eyelids in $Osr2^{-/-}$ mutant embryos (Figs. 8A–C). In contrast, no significant differences in cell proliferation in lower eyelid epithelium and mesenchyme as well as in upper eyelid mesenchyme between $Osr2^{Osr1ki/Osr1ki}$ embryos and their wild-type littermates were detected (Figs. 8D–F). However, cell proliferation in the upper eyelid epithelium of E13.5 $Osr2^{Osr1ki/Osr1ki}$ embryos was still reduced by approximately 20%, compared with the wild-type littermates (Figs. 8D–F). These data indicate that Osr2 plays an essential role in regulating eyelid outgrowth.

Osr2 function is required for maintenance of Fgf10 and Fgfr2 expression during eyelid development

The eyelid developmental defects in $Osr2^{-/-}$ mutant mice, including reduction in cell proliferation and defects in leading edge epithelial morphology, are most similar to that in mice lacking *Fgf10* (Tao et al., 2005). Thus, we examined *Fgf10* expression at different stages during eyelid development in wild-type, $Osr2^{-/-}$, and $Osr2^{Osr1ki/Osr1ki}$ mice. At E13.5, *Fgf10* mRNA was highly expressed in the central domain of the developing eyelid mesenchyme in wild-type embryos (Fig. 9A). *Fgf10* expression was dramatically reduced

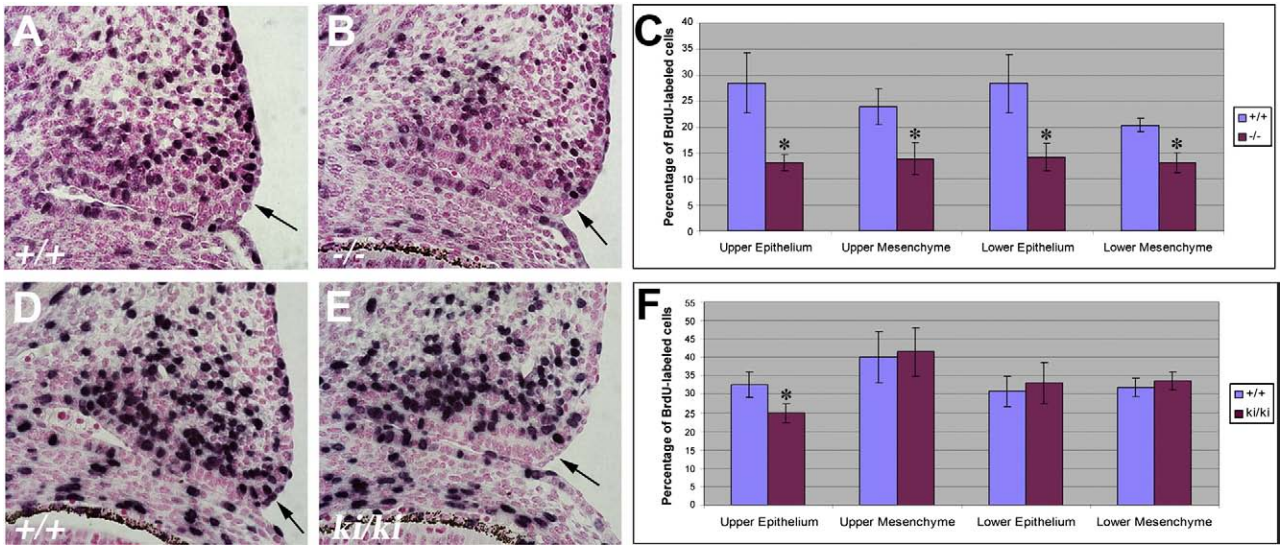

Fig. 8. Defects in cell proliferation during eyelid outgrowth in $Osr2^{-/-}$ and $Osr2^{Osr1ki/Osr1ki}$ embryos. (A, B) Sections of the upper eyelids of E13.5 wild-type (A) and $Osr2^{-/-}$ embryos labeled with BrdU (dark brown staining). Arrows point to the developing eyelids. (C) Quantitative analysis of percentage of BrdU-labeled cells. $Osr2^{-/-}$ embryos showed significant reductions in the percentage of BrdU-labeled cells, compared with the wild-type littermates, in both the epithelium and mesenchyme in the developing upper and lower eyelid tissues at E13.5. (D, E) Sections of the upper eyelids of E13.5 wild-type (D) and $Osr2^{Osr1ki/Osr1ki}$ (E) embryos labeled with BrdU. Arrows point to the developing eyelids. (F) Quantitative analysis of percentage of BrdU-labeled cells. E13.5 $Osr2^{Osr1ki/Osr1ki}$ embryos showed significant reduction in the percentage of BrdU-labeled cells, compared with the wild-type littermates, in the upper eyelid epithelium. Error bars represent standard deviations. Asterisk marks significant differences between the paired samples. $+/+$, wild-type; $-/-$, $Osr2^{-/-}$; *ki/ki*, $Osr2^{Osr1ki/Osr1ki}$ embryos.

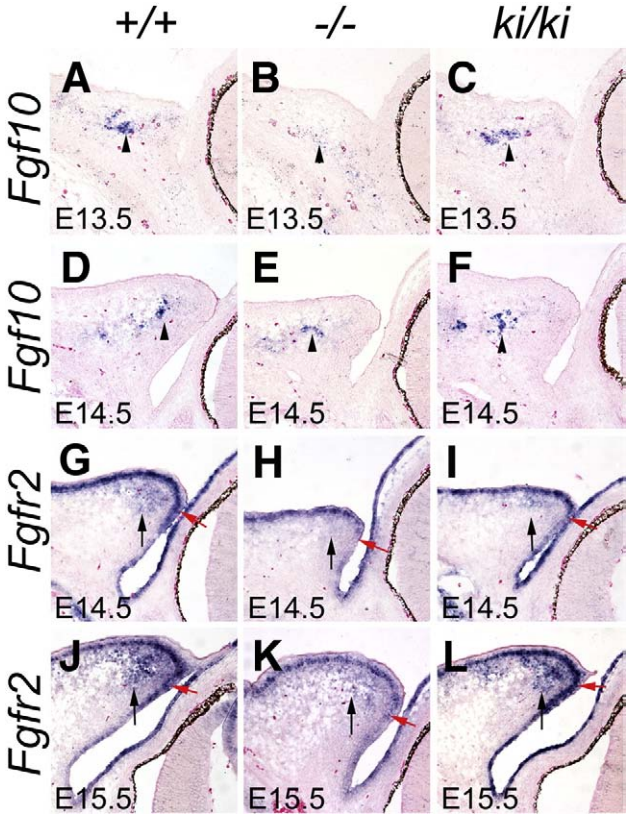

Fig. 9. Comparison of *Fgf10* and *Fgfr2* expression during eyelid development in wild-type, $Osr2^{-/-}$ and $Osr2^{Osr1ki/Osr1ki}$ mice. (A–C) *Fgf10* mRNA expression in the E13.5 upper eyelids in wild-type (A), $Osr2^{-/-}$ (B) and $Osr2^{Osr1ki/Osr1ki}$ (C) embryos. Arrowheads point to corresponding domains of *Fgf10*-expressing eyelid mesenchyme. (D–F) *Fgf10* mRNA expression in the E14.5 upper eyelids in wild-type (D), $Osr2^{-/-}$ (E) and $Osr2^{Osr1ki/Osr1ki}$ (F) embryos. Arrowheads point to the corresponding domains *Fgf10*-expressing eyelid mesenchyme. (G–I) *Fgfr2* mRNA expression in the E14.5 upper eyelids in wild-type (G), $Osr2^{-/-}$ (H) and $Osr2^{Osr1ki/Osr1ki}$ (I) embryos. Note the reduced expression of *Fgfr2* in the eyelid epithelium (red arrows) and mesenchyme (black arrows) in $Osr2^{-/-}$ (H) and $Osr2^{Osr1ki/Osr1ki}$ (I) embryos, compared with the wild-type embryo (G) at this stage. (J–L) *Fgfr2* mRNA expression in the E15.5 upper eyelids in wild-type (J), $Osr2^{-/-}$ (K) and $Osr2^{Osr1ki/Osr1ki}$ (L) embryos. *Fgfr2* expression was significantly decreased in the eyelid epithelium (red arrows) and mesenchyme (black arrows) in the $Osr2^{-/-}$ (K) embryo, compared with the wild-type embryo at this stage. In contrast, $Osr2^{Osr1ki/Osr1ki}$ embryos (L) had restored *Fgfr2* expression in both the epithelium (red arrow) and mesenchyme (black arrow) of the developing eyelids at E15.5. +/+, wild-type; −/−, $Osr2^{-/-}$; *ki/ki*, $Osr2^{Osr1ki/Osr1ki}$ embryos.

in the eyelid mesenchyme of $Osr2^{-/-}$ mutant littermates (Fig. 9B). In contrast, *Fgf10* mRNA expression in the eyelid mesenchyme in E13.5 $Osr2^{Osr1ki/Osr1ki}$ embryos (Fig. 9C) was similar to that in the wild-type embryos (Fig. 9A). At E14.5, the $Osr2^{-/-}$ embryos continued to show significantly lower levels of *Fgf10* mRNA expression in the developing eyelid mesenchyme than that in wild-type littermates (Figs. 9D, E), while the $Osr2^{Osr1ki/Osr1ki}$ embryos exhibited similar levels of *Fgf10* expression in the developing eyelid mesenchyme to that in wild-type embryos (Figs. 9D, F). These data indicate that Osr2 regulates *Fgf10* mRNA expression during eyelid development.

Fgf10 most likely signals through the Fgfr2 receptor to regulate eyelid development, since Fgfr2 is also required for eyelid outgrowth (De Moerlooze et al., 2000; Li et al., 2001). Interestingly, although *Fgfr2* expression was similar in the developing eyelid tissues in $Osr2^{-/-}$ and wild-type littermates at E13.5 (data not shown), decreased *Fgfr2* expression in both the epithelium and mesenchyme of the developing eyelid was consistently detected in $Osr2^{-/-}$ mutant embryos at E14.5 (Figs. 9G, H). *Fgfr2* expression was also reduced in both the eyelid epithelium and mesenchyme in $Osr2^{Osr1ki/Osr1ki}$ embryos at E14.5, compared with the wild-type embryos (Figs. 9G, I). At E15.5, $Osr2^{-/-}$ mice still exhibited significantly reduced *Fgfr2* expression in the developing eyelids (Fig. 9K), compared with that in wild-type littermates (Fig. 9J). However, *Fgfr2* expression is restored to wild-type levels in both the epithelium and mesenchyme of the developing eyelids in $Osr2^{Osr1ki/Osr1ki}$ mice at E15.5 (Fig. 9L), which correlated with the delayed leading edge epithelial morphogenesis in these mice. These data indicate that Osr2 controls eyelid development, at least in part, through regulation of *Fgf10* and *Fgfr2* expression.

Discussion

We previously showed that targeted deletion of the *Osr2* gene resulted in cleft palate and open eyelids at birth in $Osr2^{-/-}$ homozygous mutant mice (Lan et al., 2004). Interestingly, whereas *Osr2* is expressed in a graded pattern along the medial–lateral axis of the vertically growing palatal shelves, with lower levels of expression in the medial side than in the lateral side of the palatal mesenchyme, the $Osr2^{-/-}$ mutant mice exhibited specific reduction in cell proliferation in the medial but not lateral half of the developing palatal shelves (Lan et al., 2001, 2004). *Osr1* mRNA is expressed at relatively low abundance in the early developing palatal mesenchyme and becomes restricted to only the lateral half of the palatal mesenchyme. Thus, the palatal mesenchyme proliferation defect in the $Osr2^{-/-}$ mutant embryos was restricted to the domain of the palatal mesenchyme that normally only expressed *Osr2* but not *Osr1* mRNA (Lan et al., 2004). Similarly, the eyelid defects in the $Osr2^{-/-}$ mutant mice also correlate with distinct expression patterns between *Osr1* and *Osr2* during eyelid development (this report). No apparent defects were detected in the $Osr2^{-/-}$ mutant mice in tissues that normally express both *Osr1* and *Osr2*, including the developing kidney, limb and the proximal mandible (Lan et al., 2004). These data suggest that Osr1 and Osr2 may function redundantly during mouse embryonic development. However, the early embryonic lethality of the $Osr1^{-/-}$ mutant mice (Wang et al., 2005) precludes detailed analysis of possible functional redundancy between *Osr1* and *Osr2* in the double null mutant mice.

Functional equivalence between Osr1 and Osr2 during mouse development

To directly analyze whether Osr1 can carry out all developmental functions of Osr2 when expressed under the regulatory sequences of the *Osr2* locus, we generated mice in which the *Osr2* coding sequence is replaced by a *Myc-Osr1* cDNA cassette. We found that expression of *Myc-Osr1* from the *Osr2* locus completely rescued the cleft palate, supernumerary tooth, and tympanic ring defects of the $Osr2^{-/-}$ mutant mice. The only defect of the $Osr2^{-/-}$ mutant mice not completely rescued by the $Osr2^{Osr1ki}$ allele is the open-eyelids at birth phenotype. We found that *Myc-Osr1* expression in the $Osr2^{Osr1ki}$ mice did not completely recapitulate the endogenous *Osr2* mRNA expression patterns during eyelid development, most likely due to deletion of eyelid-specific regulatory sequences in the intronic regions of the *Osr2* locus. Moreover, we show that the $Osr2^{Osr2Aki}$ mice, which differ from the $Osr2^{Osr1ki}$ mice only in the replacement cDNA cassette, phenocopy the $Osr2^{Osr1ki}$ mice. The open eyelid phenotypes in the single homozygous and transheterozygous knockin mice further indicate that failure of the respective knockin alleles to completely rescue the eyelid developmental defects of $Osr2^{-/-}$ mutant mice is not due to the structural differences between Osr1 and Osr2A proteins. To the contrary, these data indicate that Osr1 and Osr2A have equivalent functions, when expressed under the control of the regulatory sequences of the *Osr2* gene, during mouse development.

Our finding that Osr1 and Osr2A function equivalently during mouse development is in contrast to previous reports of largely distinct functions of the *Drosophila* Odd-skipped family members (Nusslein-Volhard and Wieschaus, 1980; Coulter et al., 1990; Wang

and Coulter, 1996; Green et al., 2002; de Celis Ibeas and Bray, 2003; Johansen et al., 2003; Hatini et al., 2005). During *Drosophila* embryogenesis, *odd* and its cognate genes *sob* and *drm* are expressed in almost identical patterns (Hart et al., 1996; Johansen et al., 2003), but *odd* and *drm* mutants display completely distinct phenotypes whereas no *sob* mutation has been isolated and no synergism was detected in the compound triple mutants (Nusslein-Volhard and Wieschaus, 1980; Coulter et al., 1990; Wang and Coulter, 1996; Green et al., 2002; Johansen et al., 2003). The *odd*, *sob*, and *drm* genes are clustered together within a 200 kb genomic region and their near identical expression patterns suggest that they share regulatory enhancer sequences. However, their gene structures and protein products have diverged substantially such that the only structural similarity in the family is limited to the zinc finger motifs. The C2H2 zinc fingers in the Odd-skipped family proteins are typically involved in sequence-specific DNA binding, consistent with the proposed roles of these factors as transcriptional regulators. Indeed, both *Drosophila* ODD and mouse Osr2 have recently been shown to bind to similar specific DNA sequences (Meng et al., 2005; Kawai et al., 2007). In addition, both BOWL and DRM have been shown to directly bind to the LINES protein through their first zinc finger motif (Green et al., 2002; Hatini et al., 2005). Thus, the Odd-skipped family proteins share some functional similarities at the molecular level because of their conserved zinc finger motifs, which explains why ectopic over-expression of *odd*, *sob*, and *drm* during *Drosophila* tissue morphogenesis sometimes resulted in similar developmental effects (Green et al., 2002; Hao et al., 2003; de Celis Ibeas and Bray, 2003; Hatini et al., 2005; Bras-Pereira et al., 2006), whereas the distinct mutant phenotypes likely reflect their functional divergence from the distinct protein structures outside of the conserved zinc finger motifs.

Phylogenetic analysis indicated that two *odd-skipped* family genes were present in an ancestral metazoan, which further duplicated in the arthropod clade and gave rise to the four cognate genes in *Drosophila* (Buckley et al., 2004). In contrast, mammalian Osr1 and Osr2 share extensive amino acid sequence similarity throughout their entire length of the protein products (Lan et al., 2001), suggesting that these two genes arose by a more recent duplication from one of the ancestral *odd-skipped* genes, with apparent loss of the other, during metazoan evolution (Buckley et al., 2004). Many other paralogous transcription factors exist in mammals as pairs or groups that apparently arose by gene duplication early during vertebrate evolution (e.g., Noll, 1993; Hanks et al., 1995; Greer et al., 2000; Singh and Hannenhalli, 2008). These transcription factor paralogs often share significant structural similarities and partially overlapping expression patterns. Several examples exist where similar gene replacement strategies have been used to evaluate possible functional equivalence of closely related transcription factors in mice (e.g., Hanks et al., 1995; Bouchard et al., 2000a,b; Coppola et al., 2005; Kellerer et al., 2006). Whereas some transcription factor paralogs have been found functionally interchangeable, such as between En1 and En2 as well as between Pax2 and Pax5 (Hanks et al., 1995; Bouchard et al., 2000a,b), others showed only partial functional overlap, such as between Phox2a and Phox2b as well as between Sox8 and Sox10 (Coppola et al., 2005; Kellerer et al., 2006). By studying a large collection of human paralogous transcription factor pairs, Singh and Hannenhalli (2008) concluded that paralogous transcription factors diversify their functions mainly through divergence in either their DNA binding site motifs or in expression. Our finding that expression of *Osr1* from the *Osr2* locus rescued the developmental defects of $Osr2^{-/-}$ mutant mice indicates that the mammalian *Osr1* and *Osr2* genes evolved distinct developmental roles mainly through divergence of the *cis* regulatory sequences controlling their spatiotemporal expression rather than changes in their coding sequences. Because *Osr1* and *Osr2* are co-expressed during many developmental processes, including craniofacial, kidney, limb, and synovial joint development (Lan et al., 2001, 2004; Stricker et al., 2006), further studies using conditional gene inactivation approaches are warranted for the elucidation of the roles of *Osr1* and *Osr2* in these developmental processes.

Our findings that either *Osr1* or *Osr2A*, when expressed from the endogenous *Osr2* locus, rescued almost all developmental defects of $Osr2^{-/-}$ mice seem at odds with previously reported opposite transcriptional activity for Osr2A and Osr2B *in vitro* (Kawai et al., 2005). However, although both Osr1 and Osr2B contain only three zinc finger repeats while Osr2A contains five, our study does not directly compare the functions of Osr2A and Osr2B *in vivo*. It is possible that the $Osr2^{Osr2Aki/Osr2Aki}$ mice may have subtle cellular or physiological deficits that could be attributed to lack of the Osr2B isoform. It is also possible that the different transcriptional activity found in the cell culture assays represents non-physiological activity. In this regard, it is noteworthy, while genetic analyses in *Drosophila* indicated a primarily transcriptional repressor function for Odd-skipped (Mullen and DiNardo, 1995; DiNardo and O'Farrell, 1987; Kuhn et al., 2000; Bouchard et al., 2000a,b), its overexpression in embryos showed a role in activation (Saulier-Le Drean et al., 1998).

The roles of Osr2 in eyelid development

Our characterization of the open eyelid defects in $Osr2^{-/-}$ and $Osr2^{Osr1ki/Osr1ki}$ mice revealed an essential role for Osr2 in regulating eyelid outgrowth. Previous studies indicated that eyelid outgrowth is controlled by Fgf10–Fgfr2 signaling. Fgfr2 exists in two major isoforms, with Fgfr2b expressed primarily in the epithelium and Fgfr2c primarily in the mesenchyme, due to alternative splicing (Ornitz et al., 1996). Fgfr2b function in the epithelium is required for eyelid initiation (De Moerlooze et al., 2000; Li et al., 2001). A major ligand for the epithelial Fgfr2b receptor during eyelid development is Fgf10, which is expressed in the mesenchyme (Tao et al., 2005). Mice lacking *Fgf10* exhibited morphological and cell proliferation defects during eyelid development that are highly similar to that in the $Osr2^{-/-}$ mice (Tao et al., 2005), including reduction in eyelid epithelial cell proliferation and leading edge morphogenesis. We found that *Fgf10* expression in the developing eyelid mesenchyme was dramatically reduced in the $Osr2^{-/-}$ mutant embryos by E13.5, compared with that in their wild-type littermates, indicating that Osr2 is involved in the regulation of *Fgf10* expression during eyelid outgrowth. That decreased *Fgf10* expression is at least part of the mechanism underlying eyelid growth defects in $Osr2^{-/-}$ mice is supported by the correlation of restoration of *Fgf10* expression with the partial rescue of eyelid growth in the $Osr2^{Osr1ki/Osr1ki}$ mice.

Interestingly, *Fgfr2* expression was affected in the $Osr2^{-/-}$ mutant mice after E13.5. It is possible that the reduction in *Fgfr2* expression is a secondary effect of *Fgf10* down-regulation during eyelid development in the $Osr2^{-/-}$ mutant mice. However, *Fgfr2* expression in the $Osr2^{Osr1ki/Osr1ki}$ embryos was also reduced, which correlated with incomplete recapitulation of endogenous *Osr2* gene expression, in particular in the inner eyelid epithelium, suggesting that Osr2 may also play a primary role in maintaining *Fgfr2* expression during eyelid development. In the $Osr2^{Osr1ki/Osr1ki}$ mice, although the leading edge epithelium of the developing eyelids formed periderm ridges that migrated over the developing corneal surface, the eyelids failed to fuse in the central regions due to the delayed eyelid development prior to E15.5. Further elucidation of the roles of the Osr1 and Osr2 transcription factors, in particular identification of downstream target genes, will be necessary to understand how these transcription factors interact with the Fgf10–Fgfr2 and other signaling pathways during mouse development.

Acknowledgments

We thank Tom Gridley for the CJ7 mouse ES cells, Qingru Wang for technical assistance, and the University of Rochester Transgenic

Mouse Facility for assistance in generation of chimeric mice from targeted ES cells. This work was supported by NIH/NIDCR grant R01DE013681 to RJ.

References

Bouchard, M., Pfeffer, P., Busslinger, M., 2000a. Functional equivalence of the transcription factors Pax2 and Pax5 in mouse development. Development 127, 3703–3713.

Bouchard, M., St-Amand, J., Cote, S., 2000b. Combinatorial activity of pair-rule proteins on the *Drosophila* gooseberry early enhancer. Dev. Biol. 222, 135–146.

Bras-Pereira, C., Bessa, J., Casares, F., 2006. Odd-skipped genes specify the signaling center that triggers retinogenesis in *Drosophila*. Development 133, 4145–4149.

Buckley, M., Chau, J., Hoppe, P., 2004. *odd-skipped* homologs function during gut development in *C. elegans*. Dev. Genes Evol. 214, 10–18.

Coppola, E., Pattyn, A., Guthrie, S.C., Goridis, C., Studer, M., 2005. Reciprocal gene replacements reveal unique functions for Phox2 genes during neural differentiation. EMBO J. 24, 4392–4403.

Coulter, D.E., Wieschaus, E., 1988. Gene activities and segmental patterning in *Drosophila*: analysis of odd-skipped and pair-rule double mutants. Genes Dev. 2, 1812–1823.

Coulter, D.E., Swaykus, E.A., Beran-Koehn, M.A., Goldberg, D., Wieschaus, E., Schedl, P., 1990. Molecular analysis of odd-skipped, a zinc finger encoding segmentation gene with a novel pair-rule expression pattern. EMBO J. 9, 3795–3804.

de Celis Ibeas, J.M., Bray, S.J., 2003. Bowl is required downstream of Notch for elaboration of distal limb patterning. Development 130, 5943–5952.

De Moerlooze, L., Spencer-Dene, B., Revest, J.-M., Hajihosseini, M., Rosewell, I., Dickson, C., 2000. An important role for the IIIb isoform of fibroblast growth factor 2 (FGFR2) in mesenchymal-epithelial signaling during mouse organogenesis. Development 127, 483–492.

DiNardo, S., O'Farrell, P.H., 1987. Establishment and refinement of segmental pattern in the *Drosophila* embryos: spatial control of *engrailed* expression by pair-rule genes. Genes Dev. 1, 1212–1225.

Green, R.B., Hatini, V., Johansen, K.A., Liu, X.J., Lengyel, J.A., 2002. Drumstick is a zinc finger protein that antagonizes Lines to control patterning and morphogenesis of the *Drosophila* hindgut. Development 129, 3645–3656.

Greer, J.M., Puetz, J., Thomas, K.R., Capecchi, M.R., 2000. Maintenance of functional equivalence during paralogous Hox gene evolution. Nature 403, 661–664.

Hanks, M., Wurst, W., Anson-Cartwright, L., Auerbach, A.B., Joyner, A.L., 1995. Rescue of the En-1 mutant phenotype by replacement of En-1 with En-2. Science 269, 679–682.

Hao, I., Green, R.B., Dunaevsky, O., Lengyel, J.A., Rauskolb, C., 2003. The odd-skipped family of zinc-finger genes promotes *Drosophila* leg segmentation. Dev. Biol. 263, 282–295.

Hatini, V., Green, R.B., Lengyel, J.A., Bray, S.J., DiNardo, S., 2005. The Drumstick/Lines/Bowl regulatory pathway links antagonistic Hedgehog and Wingless signaling inputs to epidermal cell differentiation. Genes Dev. 19, 709–718.

Hart, M.C., Wang, L., Coulter, D.E., 1996. Comparison of the structure and expression of odd-skipped and two related genes that encode a new family of zinc finger proteins in *Drosophila*. Genetics 144, 171–182.

Holzenberger, M., Leneuve, P., Hamard, G., Ducos, B., Perin, L., Binoux, M., Le Bouc, Y., 2000. A targeted partial invalidation of the insulin-like growth factor I receptor gene in mice causes a postnatal growth deficit. Endocrinology 141, 2557–2566.

James, R.G., Kamei, C.N., Wang, Q., Jiang, R., Schultheiss, T.M., 2006. Odd-skipped related 1 is required for development of the metanephric kidney and regulates formation and differentiation of kidney precursor cells. Development 133, 2995–3004.

Johansen, K.A., Iwaki, D.D., Lengyel, J.A., 2003. Localized JAK/STAT signaling is required for oriented cell rearrangement in a tubular epithelium. Development 130, 135–145.

Katoh, M., 2002. Molecular cloning and characterization of OSR1 on human chromosome 2p24. Int. J. Mol. Med. 10, 221–225.

Kawai, S., Kato, T., Inaba, H., Okahashi, N., Amano, A., 2005. Odd-skipped related 2 splicing variants show opposite transcriptional activity. Biochem. Biophys. Res. Commun. 328, 306–311.

Kawai, S., Yamauchi, M., Wakisaka, S., Ooshima, T., Amano, A., 2007. Zinc-finger transcription factor odd-skipped related 2 is one of the regulators in osteoblast proliferation and bone formation. J. Bone Miner. Res. 22, 1362–1372.

Kellerer, S., Schreiner, S., Stolt, C.C., Scholz, S., Bosl, M.R., Wegner, M., 2006. Replacement of the Sox10 transcription factor by Sox8 reveals incomplete functional equivalence. Development 133, 2875–2886.

Kuhn, D.T., Chaverri, J.M., Persaud, D.A., Madjidi, A., 2000. Pair-rule genes cooperate to activate en stripe 15 and refine its margins during germ band elongation in the *D. melanogaster* embryo. Mech. Dev. 95, 297–300.

Lakso, M., Pichel, J.G., Gorman, J.R., Sauer, B., Okanoto, Y., Lee, E., Alt, F.W., Westphal, H., 1996. Efficient *in vivo* manipulation of mouse genomic sequences at the zygote stage. Proc. Natl. Acad. Sci. U. S. A. 93, 5860–5865.

Lan, Y., Kingsley, P.D., Cho, E.S., Jiang, R., 2001. Osr2, a new mouse gene related to *Drosophila* odd-skipped, exhibits dynamic expression patterns during craniofacial, limb, and kidney development. Mech. Dev. 107, 175–179.

Lan, Y., Ovitt, C.E., Cho, E.S., Maltby, K.M., Wang, Q., Jiang, R., 2004. Odd-skipped related 2 (Osr2) encodes a key intrinsic regulator of secondary palate growth and morphogenesis. Development 131, 3207–3216.

Li, C., Guo, H., Xu, X., Weiberg, W., Deng, C.X., 2001. Fibroblast growth factor receptor 2 (Fgfr2) plays an important role in eyelid and skin formation and patterning. Dev. Dyn. 222, 471–483.

Martin, J.F., Bradley, A., Olson, E.N., 1995. The paired-like homeobox gene Mhox is required for early events of skeletogenesis in multiple lineages. Genes Dev. 9, 1237–1249.

Meng, X., Brodsky, M.H., Wolfe, A.A., 2005. A bacterial one-hybrid system for determining the DNA-binding specificity of transcription factors. Nat. Biotechnol. 23, 988–994.

Mullen, J.R., DiNardo, S., 1995. Establishing parasegments in *Drosophila* embryos: roles of the *odd-skipped* and *naked* genes. Dev. Biol. 169, 295–308.

Noll, M., 1993. Evolution and role of *Pax* genes. Curr. Opin. Genet. Dev. 3, 595–605.

Nusslein-Volhard, C., Wieschaus, E., 1980. Mutations affecting segment number and polarity in *Drosophila*. Nature 287, 795–801.

Olson, E.N., Arnold, H.H., Rigby, P.W., Wold, B.J., 1996. Know your neighbors: three phenotypes in null mutants of the myogenic bHLH gene MRF4. Cell 85, 1–4.

Ornitz, D.M., Xu, J., Colvin, J.S., McEwen, D.G., MacArthur, C.A., Coulier, F., Gao, G., Goldfarb, M., 1996. Receptor specificity of the fibroblast growth factor family. J. Biol. Chem. 271, 15292–15297.

Rupp, R.A.W., Snider, L., Weintraub, H., 1994. *Xenopus* embryos regulate the nuclear localization of XMoyoD. Genes Dev. 8, 1311–1323.

Seidl, K.J., Manis, J.P., Bottaro, A., Zhang, J., Davidson, L., Kisselgof, A., Oettgen, H., Alt, F.W., 1999. Position-dependent inhibition of class-switch recombination by PGK-neor cassettes inserted into the immunoglobulin heavy chain constant region locus. Proc. Natl. Acad. Sci. U. S. A. 96, 3000–3005.

So, P.L., Danielian, P.S., 1999. Cloning and expression analysis of a mouse gene related to *Drosophila* odd-skipped. Mech. Dev. 84, 157–160.

Saulier-Le Drean, B., Nasiadka, A., Dong, J., Krause, H.M., 1998. Dynamic changes in the functions of *Odd-skipped* during early *Drosophila* embryogenesis. Development 125, 4851–4861.

Singh, L.N., Hannenhalli, S., 2008. Functional diversification of paralogous transcription factors via divergence in DNA binding site motif and in expression. PLos One 3, e2345.

Stricker, S., Brieske, N., Haupt, J., Mundlos, S., 2006. Comparative expression pattern of Odd-skipped related genes Osr1 and Osr2 in chick embryonic development. Gene Expr. Patterns 6, 826–834.

Swiatek, P.J., Gridley, T., 1993. Perinatal lethality and defects in hindbrain development in mice homozygous for a targeted mutation of the zinc-finger gene Krox20. Genes Dev. 7, 2071–2084.

Tao, H., Shimizu, M., Kusumoto, R., Ono, K., Noji, S., Ohuchi, H., 2005. A dual role of Fgf10 in proliferation and coordinated migration of epithelial leading edge cells during mouse eyelid development. Development 132, 3217–3230.

Wang, L., Coulter, D.E., 1996. bowel, an odd-skipped homolog, functions in the terminal pathway during *Drosophila* embryogenesis. EMBO J. 15, 3182–3196.

Wang, Q., Lan, Y., Cho, E.S., Maltby, K.M., Jiang, R., 2005. Odd-skipped related 1 (Odd 1) is an essential regulator of heart and urogenital development. Dev. Biol. 288, 582–594.